Electronic Supplementary Material (ESI) for Inorganic Chemistry Frontiers.
This journal is © the Partner Organisations 2021

Electronic Supplementary Information

A Bimetal Hierarchical Layer Structure MOF Grown on Ni Foam as Bifunctional Catalyst for OER and HER

Qiuxiang Mou, Zhenhang Xu, Guannan Wang, Erlei Li, Jinyan Liu, Pingping Zhao, Xinghai Liu, Houbin Li, and Gongzhen Cheng

Table of contents

1. Supplementary Figures

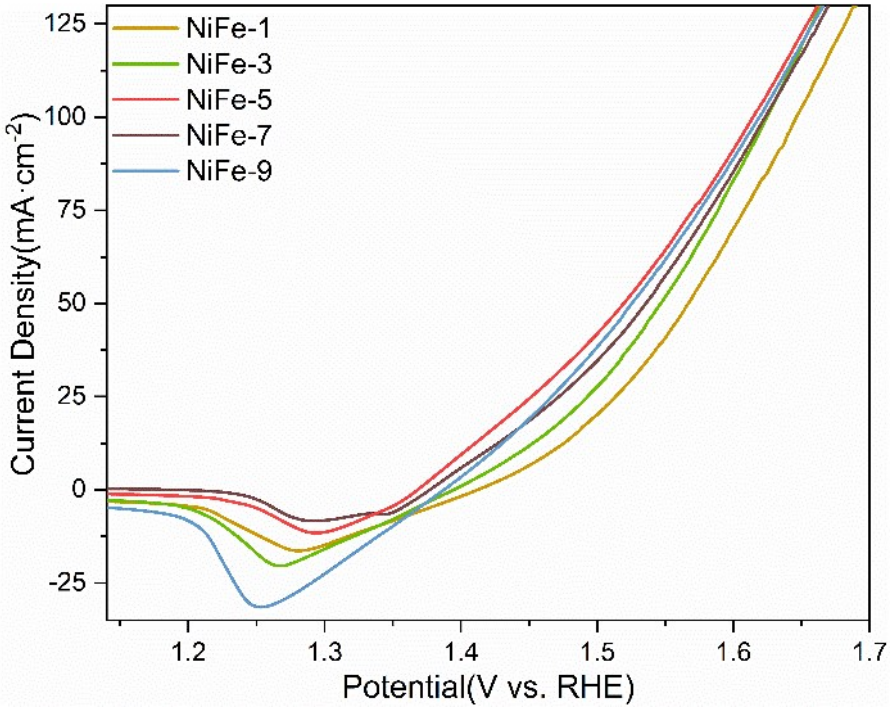

Fig. S1. LSV curves of different loading of NiFe bimetallic MOF.

Note: The NiFe-1 refers to 1.17 mmol nickel (II) nitrate hexahydrate and 0.058 mmol iron (III) nitrate nonahydrate were added in the solution to fabricate the MOF, the content of Ni^{2+} and Fe^{3+} in NiFe-α exactly equal to α times of that in NiFe-1

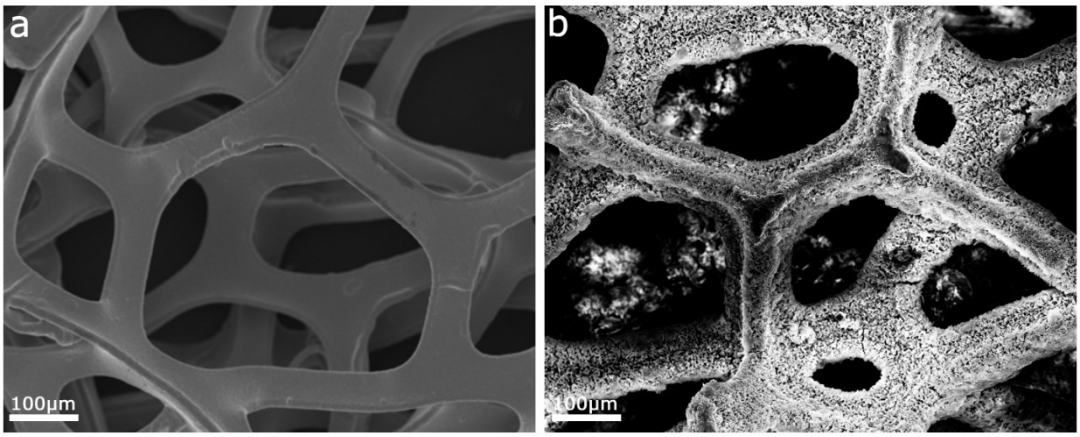

Fig. S2. SEM of nickel foam skeleton before (a) and after (b) loading the NiFe-MOF.

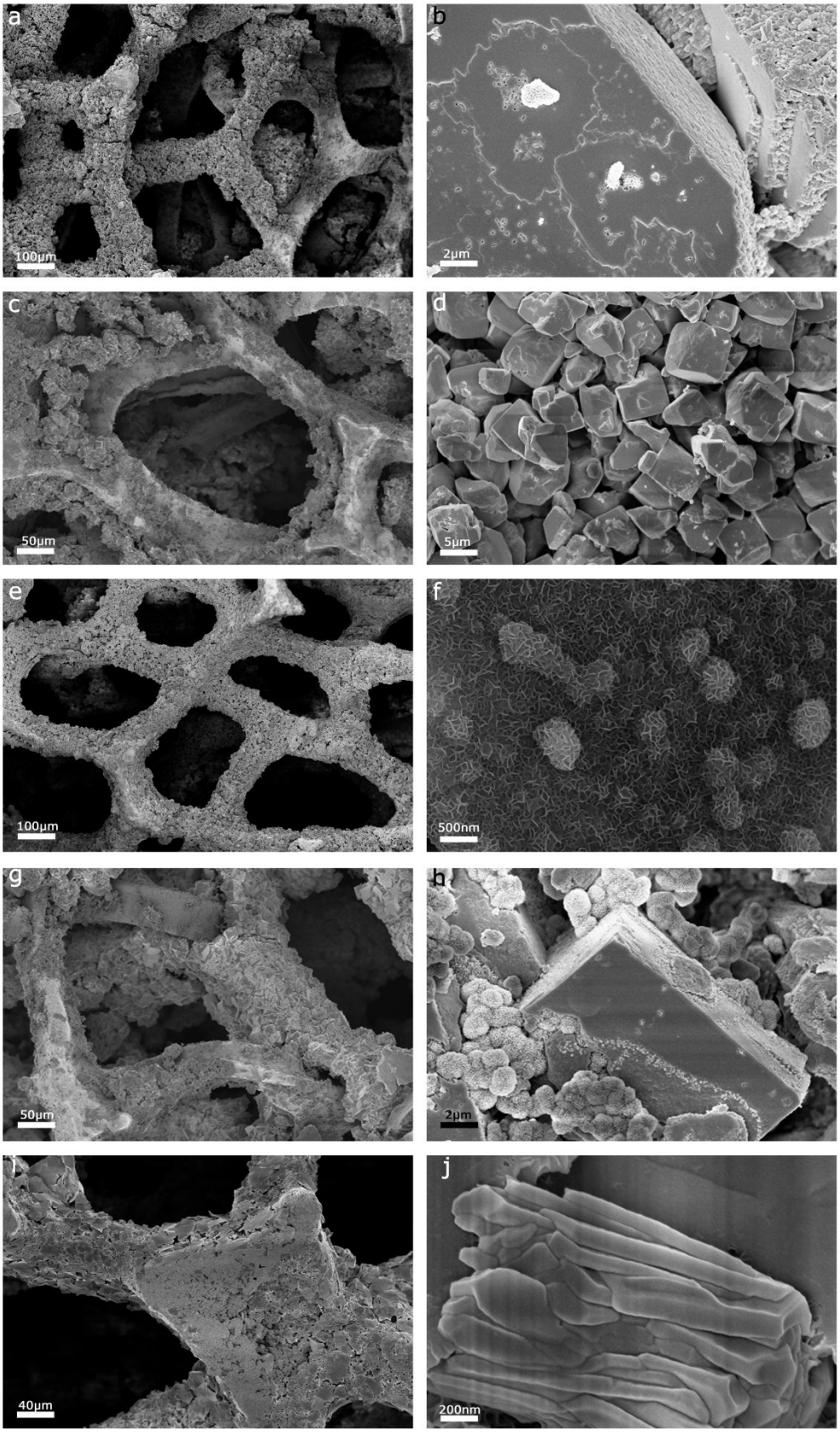

Fig. S3. SEM of (a) (b) NiFe-MOF-1, (c) (d) NiFe-MOF-3, (e) (f) NiFe-MOF-5, (g) (h) NiFe-MOF-7 and (i) (j) NiFe-MOF-9.

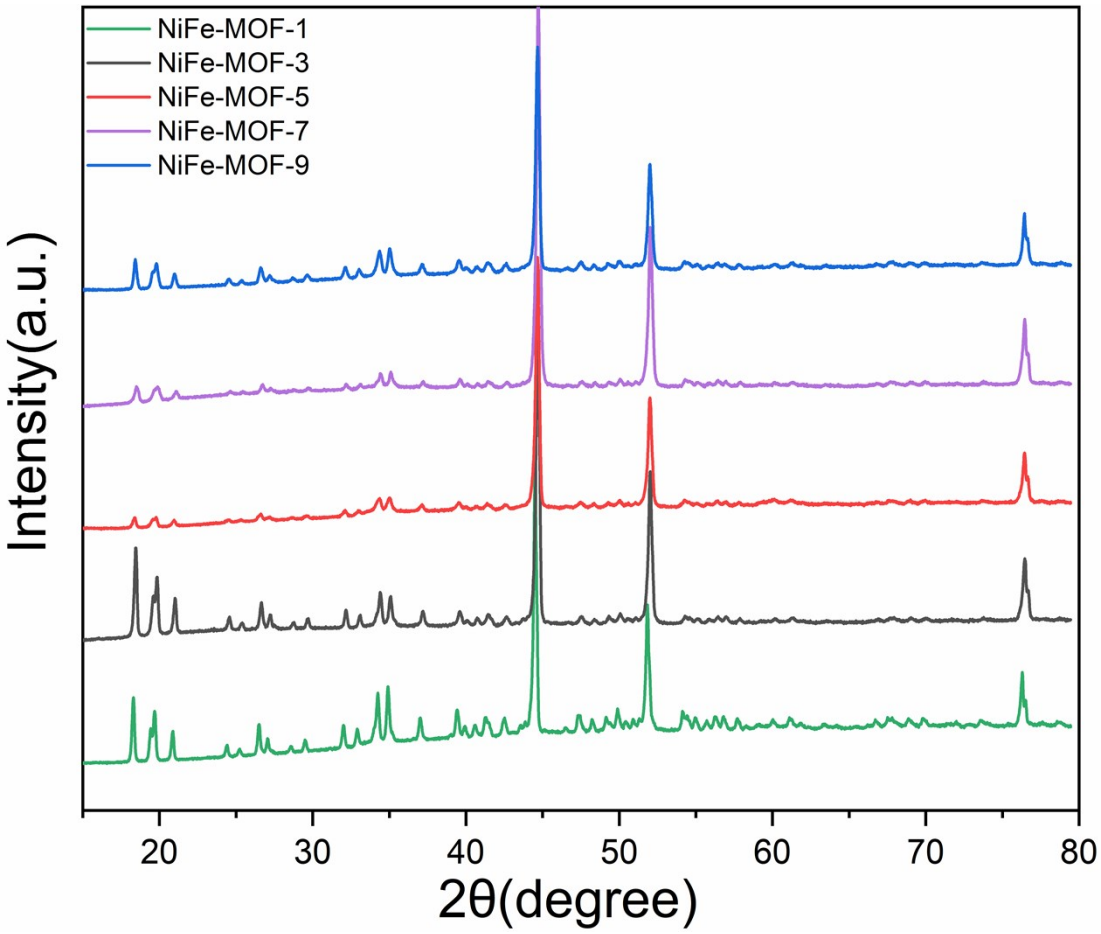

Fig. S4. XRD patterns of NiFe-MOF-α.

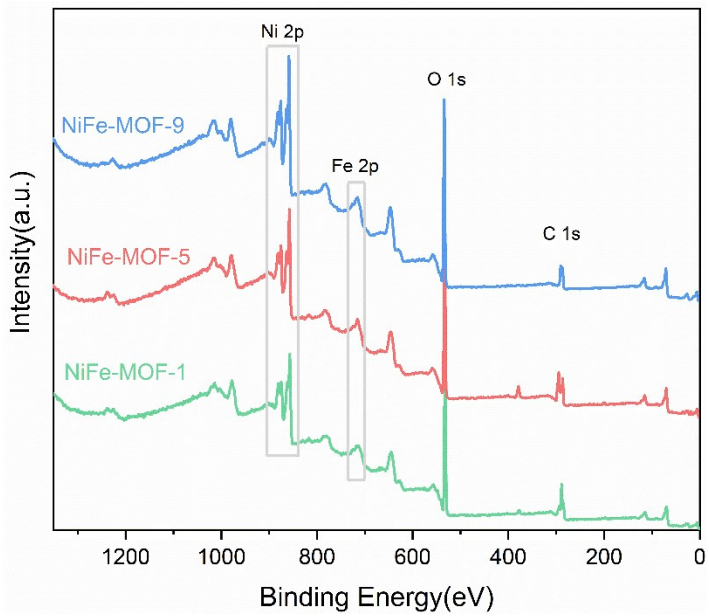

Fig. S5. The survey spectra of NiFe-MOF-1, NiFe-MOF-5, NiFe-MOF-9.

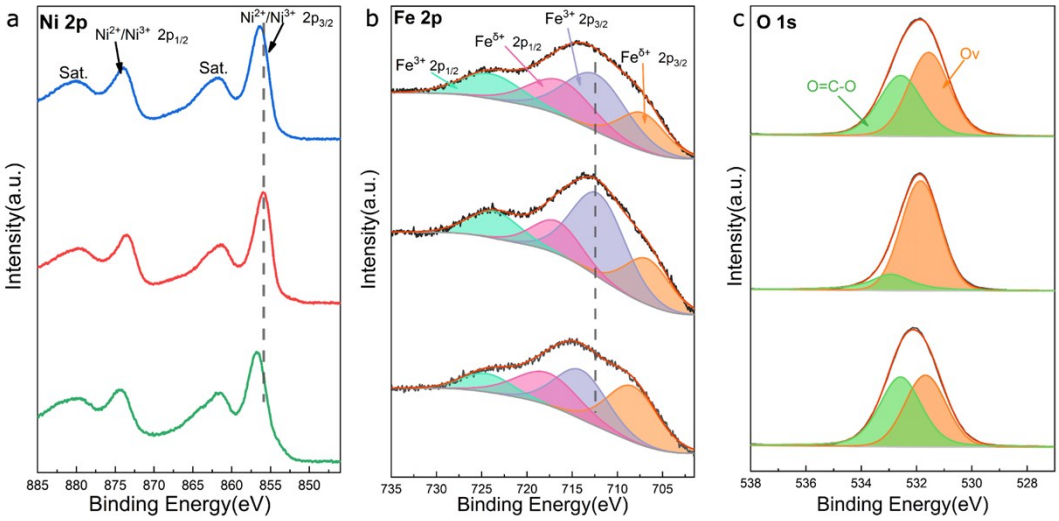

Fig. S6. High-resolution spectra of (a) Ni 2p, (b) Fe 2p, and (c) O 1s for NiFe-MOF-1 (bottom), NiFe-MOF-5 (middle) and NiFe-MOF-9 (top).

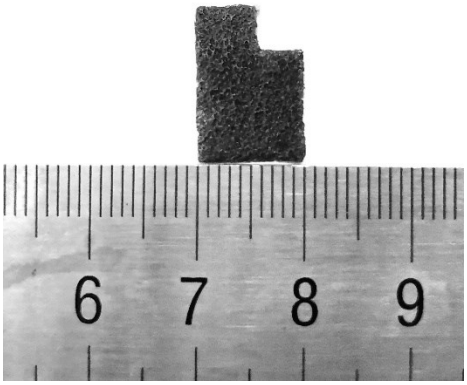

Fig. S7. The picture of NiFe-MOF-α electrodes.

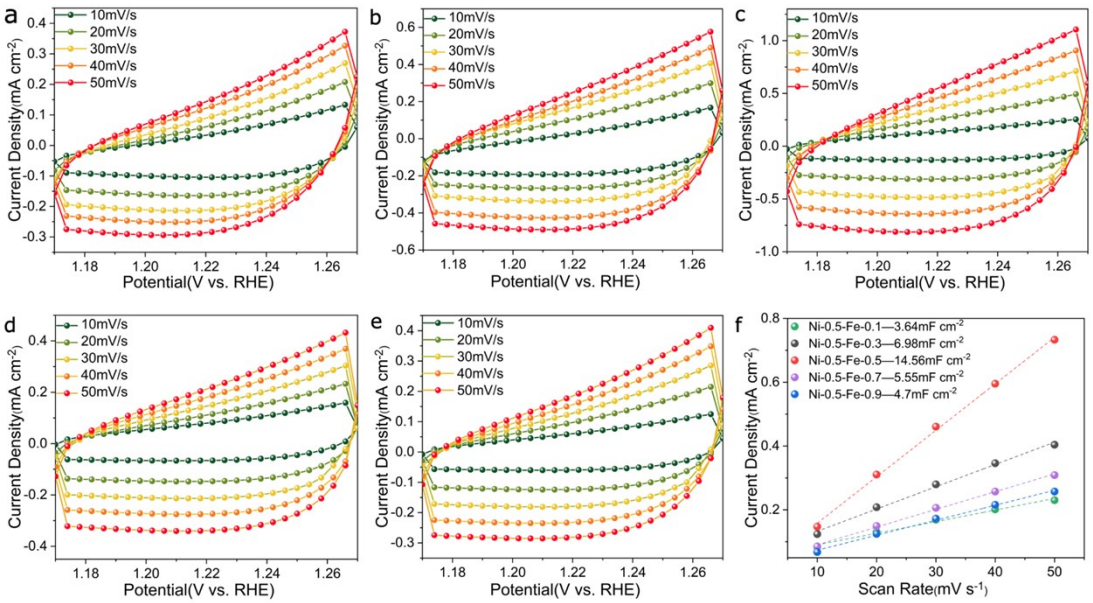

Fig. S8. CV curves of (a) NiFe-MOF-1, (b) NiFe-MOF-3, (c) NiFe-MOF-5, (d) NiFe-MOF-7, (e) NiFe-MOF-9 in 1.17-1.14 V vs RHE at different scan rate. (f) Current density differences current against the scan rate for the estimation of C_{dl}.

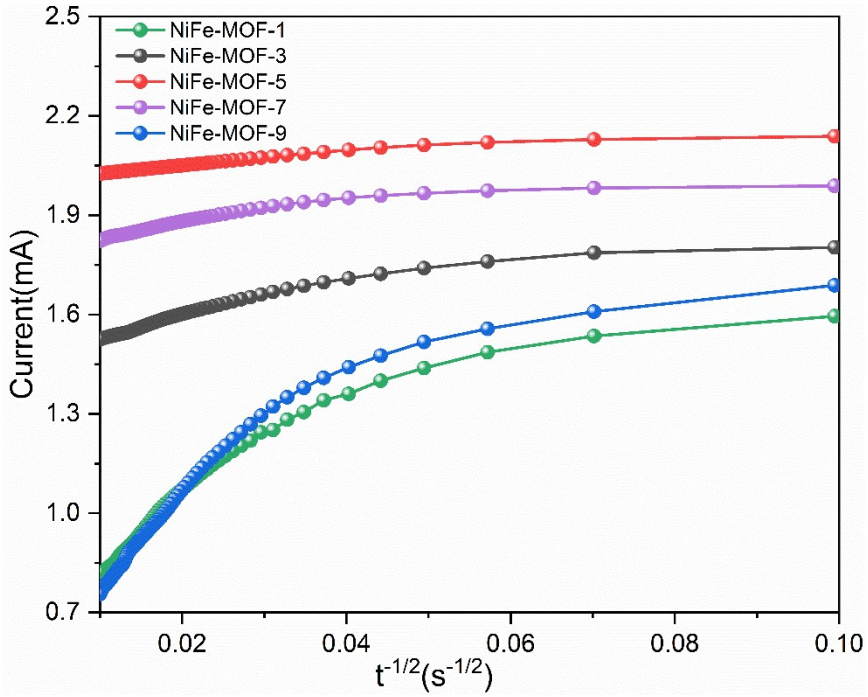

Fig. S9. Chronoamperometric measurements of the oxygen diffusion rate for NiFe-MOF-α.

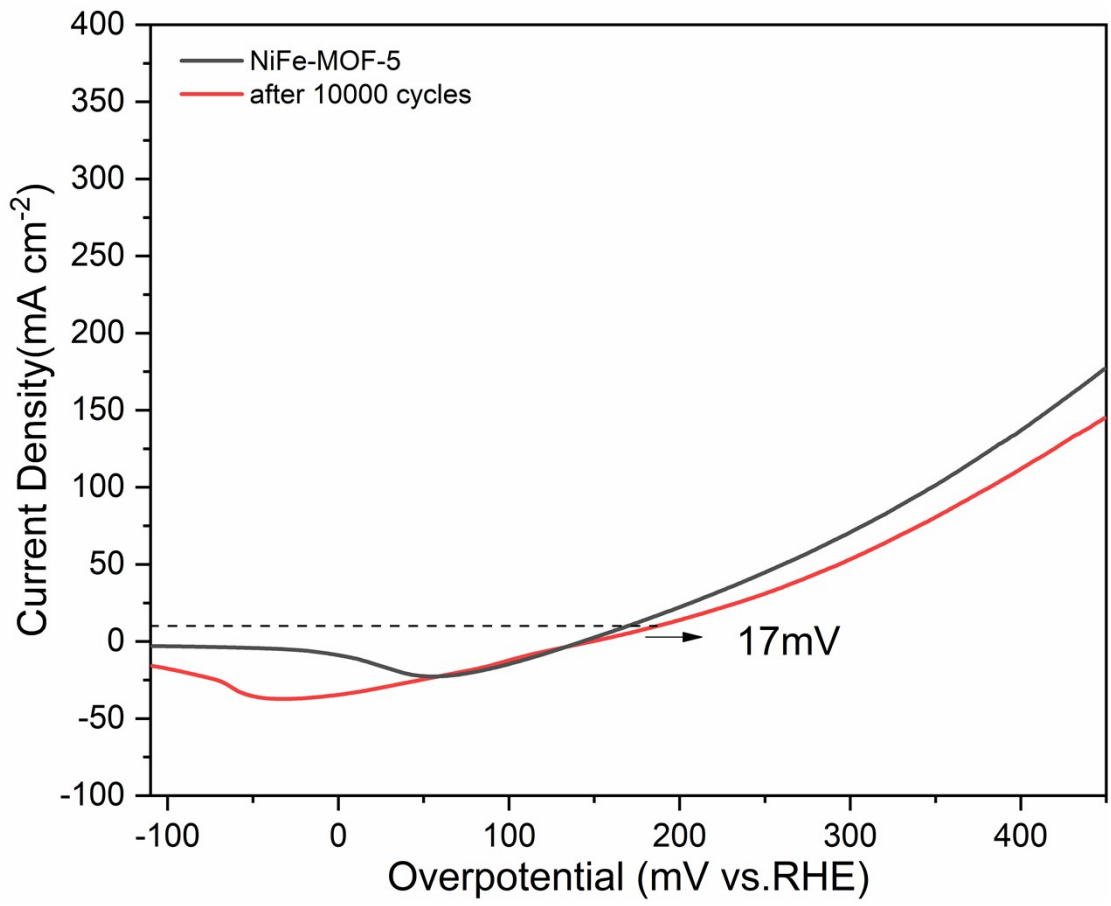

Fig. S10. Polarization curves of NiFe-MOF-5 at the 1st and 10000th cycle for OER.

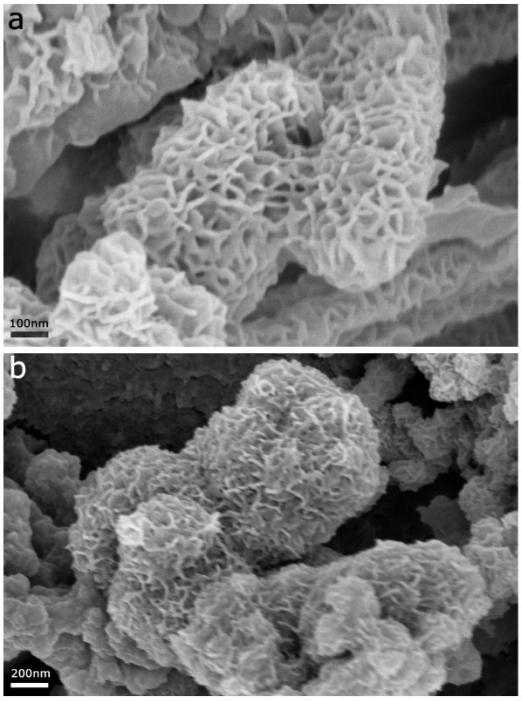

Fig. S11. SEM of NiFe-MOF-5 before (top) and after (bottom) OER.

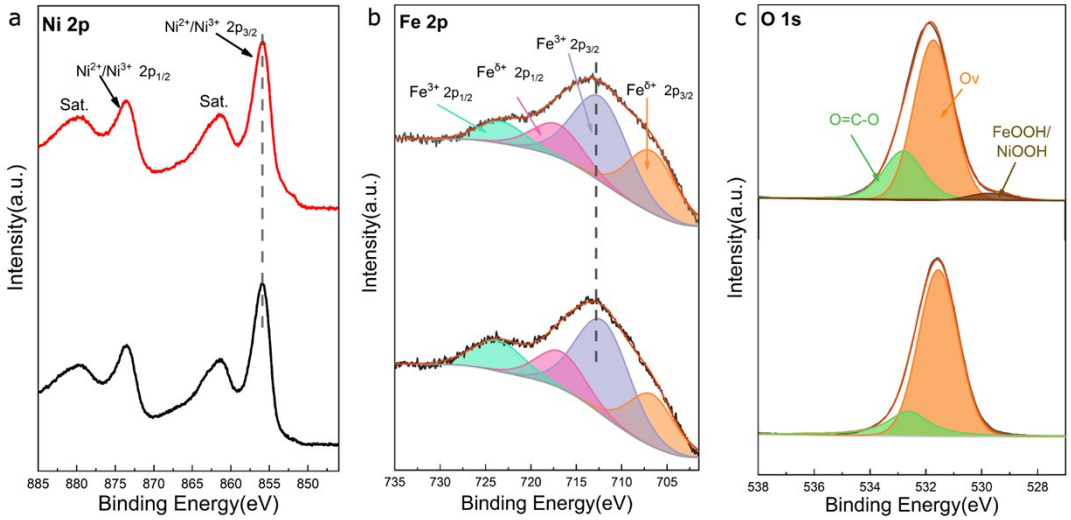

Fig. S12. (a) Ni 2p, (b) Fe 2p and (c) O 1s XPS spectra of NiFe-MOF-5 before (bottom) and after (top) OER.

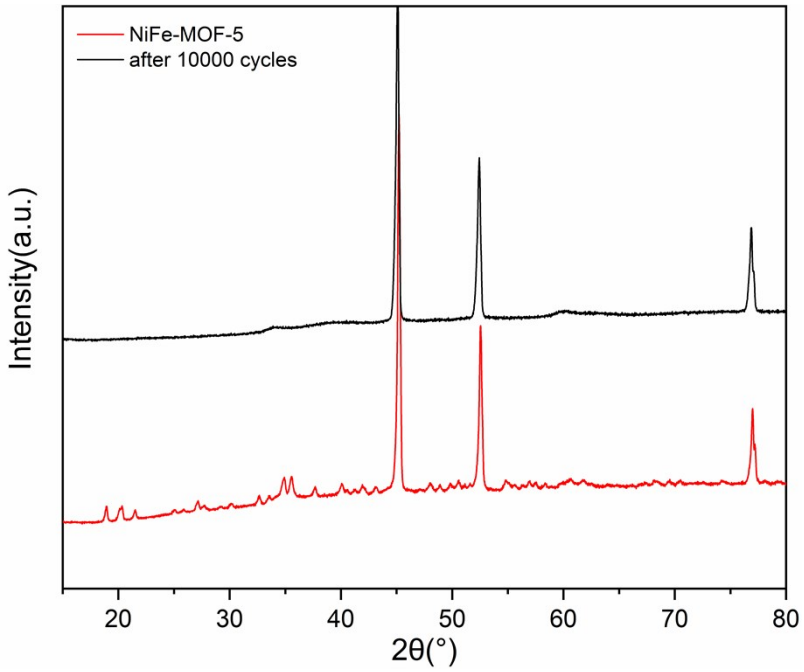

Fig. S13. XRD pattern of NiFe-MOF-5 before and after OER.

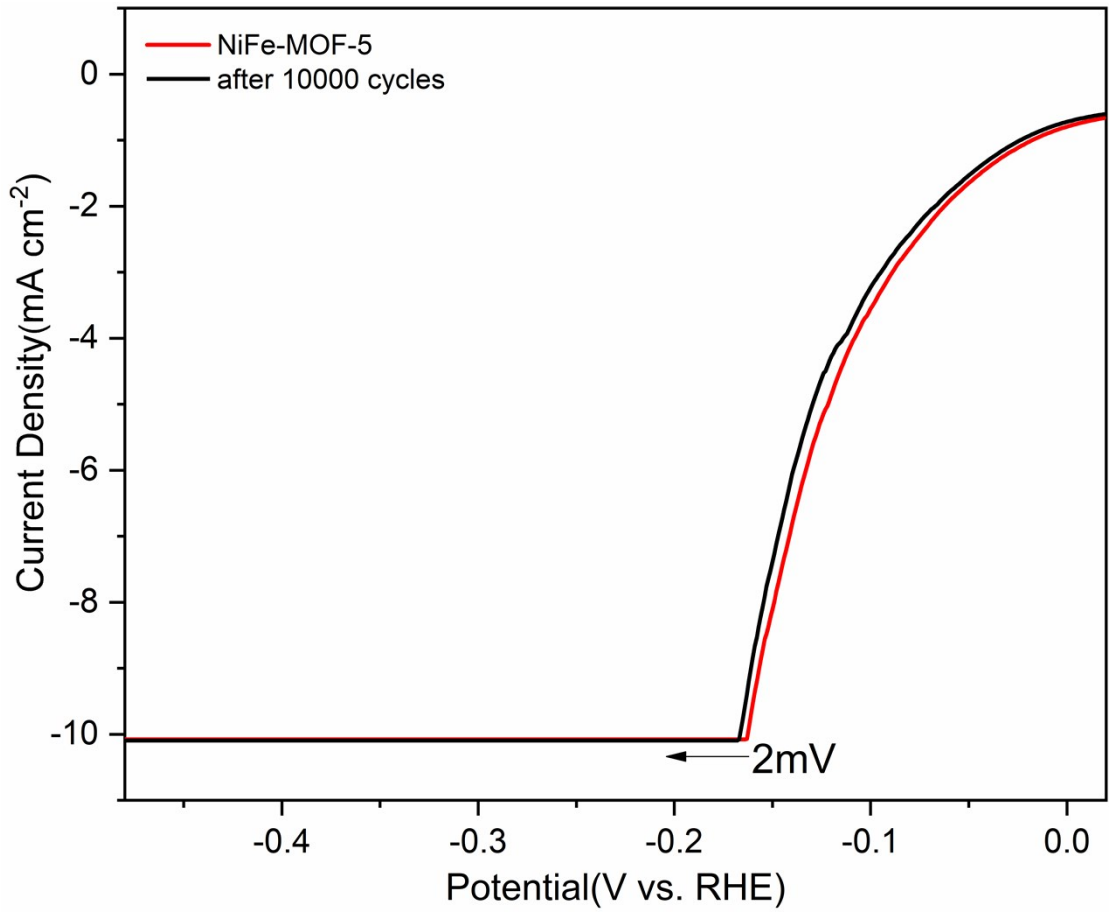

Fig. S14. Polarization curves of NiFe-MOF-5 at the 1st and 10000th cycle for HER.

2. Supplementary Tables

Table S1. The detailed information of NiFe-MOF-α with different concentration of Fe^{3+}.

Sample	n ($Ni(NO_3)_2 \cdot 6H_2O$)	n ($Fe(NO_3)_3 \cdot 6H_2O$)
NiFe-MOF-1	5.85mmol	0.058 mmol
NiFe-MOF-3	5.85mmol	0.174 mmol
NiFe-MOF-5	5.85mmol	0.29 mmol
NiFe-MOF-7	5.85mmol	0.406 mmol
NiFe-MOF-9	5.85mmol	0.522 mmol

Table S2. Percentage of different O species in NiFe-MOF-α.

Sample	O_v	O=C-O
NiFe-MOF-1	47.6%	52.4%
NiFe-MOF-5	81.7%	18.3%
NiFe-MOF-9	55.4%	44.6%

Table S3. Comparison of OER performance of NiFe-MOF-5 with reported Electrocatalysts.

Catalyst	η(mV) at 10 mA cm^{-2}	Tafel Slope (mV dec^{-1})	Electrolyte	Reference
NiFe-MOF-5	168	42	1 M KOH	This work
NiFe LDH/$NiCo_2O_4$	290	53	1 M KOH	[1]
Fe@Ni HNSs	220	53	1 M KOH	[2]
Fe-CoNi-OH	210	28	1 M KOH	[3]
$(Ni_2Co_1)_{0.925}Fe_{0.075}$-MOF-NF	257	41.3	1 M KOH	[4]
$Co_{1.6}Ni_{0.4}P_4O_{12}$-C	230	51.1	1 M KOH	[5]
NiO/Co_3O_4	262	58	1 M KOH	[6]
Co_2P/CoNPC	326	72.6	1 M KOH	[7]
Fe_2-GNCL	355	66	1 M KOH	[8]
Ni-N_4/GHSs/Fe-N_4	390	81	0.1 M KOH	[9]
MoS_2/rFe-$NiCo_2O_4$	270	39	1 M KOH	[10]
Ni–Fe LDH@NiCu	218	56.9	1 M KOH	[11]
FeOOH/Ni_3N	244	65	1 M KOH	[12]
Fe_2P-NiP_2@PC	248	54	1 M KOH	[13]
$Ni_{0.75}Fe_{0.25}$-P/PO_3@fCNT	239	34.4	1 M KOH	[14]
(Ni, Fe)S_2@MoS_2	270	43.21	1 M KOH	[15]
NCMC	290	73	1 M KOH	[16]
Ni_2P-VP_2/NF	220	49	1 M KOH	[17]
NM50-Ni_3S_4/NF	257	67	1 M KOH	[18]
Ni-Fe-2	219	53	1 M KOH	[19]
$NiCo_2S_4$-4	243	54.9	1 M KOH	[20]

Table S4. The normalized oxygen diffusion coefficients (D) of NiFe-MOF-α.

Catalyst	NiFe-MOF-1	NiFe-MOF-3	NiFe-MOF-5	NiFe-MOF-7	NiFe-MOF-9
Normalized D	1	1.8	3.54	2.77	1.59

Table S5. Comparison of overall water splitting performance of NiFe-MOF-5 with reported materials.

Catalyst	**η(V) at 10 mA cm^{-2}**	**Electrolyte**	**Reference**
NiFe-MOF-5	1.57	1 M KOH	This work
CoP NFs	1.65	1 M KOH	[21]
CoFe@NiFe/NF	1.59	1 M KOH	[22]
NCMC	1.63	1 M KOH	[16]
$NiCo_2S_4$	1.58	1 M KOH	[20]
CoFeO@BP	1.58	1 M KOH	[23]
NiFe LDH/$NiCo_2O_4$/NF	1.60	1 M KOH	[1]
FeOOH/Ni_3N	1.58	1 M KOH	[12]
Co_1–Fe_1–B–P	1.68	1 M KOH	[24]
Ni_3S_2	1.63	1 M KOH	[25]
FeNiOH/NF	1.67	1 M KOH	[26]
O-CoMoS	1.60	1 M KOH	[27]
Co_3S_4@MoS_2	1.58	1 M KOH	[28]
$P_{8.6}$-Co_3O_4/NF	1.63	1 M KOH	[29]
$Co_5Mo_{1.0}O$ NSs@NF	1.68	1 M KOH	[30]
$Ni_{0.75}Fe_{0.125}V_{0.125}$-LDHs/NF	1.591	1 M KOH	[31]
NiS/Ni2P/CC	1.67	1 M KOH	[32]
$Fe_{11\%}$-NiO/NF	1.579	1 M KOH	[33]
S-$NiFe_2O_4$/NF	1.65	1 M KOH	[34]
$NiCo_2S_4$@NiFe LDH	1.60	1 M KOH	[35]

3. Reference

1 Z. Wang, S. Zeng, W. Liu, X. Wang, Q. Li, Z. Zhao and F. Geng, Coupling Molecularly Ultrathin Sheets of NiFe-Layered Double Hydroxide on $NiCo_2O_4$ Nanowire Arrays for Highly Efficient Overall Water-Splitting Activity, *ACS Appl. Mater. Interfaces*, 2017, **9**, 1488-1495.

2 Y. Ding, B.-Q. Miao, Y. Zhao, F.-M. Li, Y.-C. Jiang, S.-N. Li and Y. Chen, Direct growth of holey Fe_3O_4-coupled $Ni(OH)_2$ sheets on nickel foam for the oxygen evolution reaction, *Chinese J. Catal.*, 2021, **42**, 271-278.

3 C. Huang, Y. Zhong, J. Chen, J. Li, W. Zhang, J. Zhou, Y. Zhang, L. Yu and Y. Yu, Fe induced nanostructure reorganization and electronic structure modulation over CoNi (oxy)hydroxide nanorod arrays for boosting oxygen evolution reaction, *Chem. Eng. J.*, 2021, **403**, 126304.

4 Q. Qian, Y. Li, Y. Liu, L. Yu and G. Zhang, Ambient Fast Synthesis and Active Sites Deciphering of Hierarchical Foam-Like Trimetal-Organic Framework Nanostructures as a Platform for Highly Efficient Oxygen Evolution Electrocatalysis, *Adv. Mater.*, 2019, **31**, e1901139.

5 Y. Li, Z. Wang, J. Hu, S. Li, Y. Du, X. Han and P. Xu, Metal–Organic Frameworks Derived Interconnected Bimetallic Metaphosphate Nanoarrays for Efficient Electrocatalytic Oxygen Evolution, *Adv. Funct. Mater.*, 2020, **30**, 1910498.

6 J. Zhang, J. Qian, J. Ran, P. Xi, L. Yang and D. Gao, Engineering Lower Coordination Atoms onto NiO/Co_3O_4 Heterointerfaces for Boosting Oxygen Evolution Reactions, *ACS Catal.*, 2020, **10**, 12376-12384.

7 H. Liu, J. Guan, S. Yang, Y. Yu, R. Shao, Z. Zhang, M. Dou, F. Wang and Q. Xu, Metal-Organic Framework-Derived Co_2P Nanoparticle/Multi-Doped Porous Carbon as a Trifunctional Electrocatalyst, *Adv. Mater.*, 2020, DOI: 10.1002/adma.202003649, e2003649.

8 Y. S. Wei, L. Sun, M. Wang, J. Hong, L. Zou, H. Liu, Y. Wang, M. Zhang, Z. Liu, Y. Li, S. Horike, K. Suenaga and Q. Xu, Fabricating Dual-Atom Iron Catalysts for Efficient Oxygen Evolution Reaction: A Heteroatom Modulator Approach, *Angew. Chem. Int. Ed. Engl.*, 2020, **59**, 16013-16022.

9 J. Chen, H. Li, C. Fan, Q. Meng, Y. Tang, X. Qiu, G. Fu and T. Ma, Dual Single-Atomic $Ni-N_4$ and $Fe-N_4$ Sites Constructing Janus Hollow Graphene for Selective Oxygen Electrocatalysis, *Adv. Mater.*, 2020, DOI: 10.1002/adma.202003134, e2003134.

10 J. Li, D. Chu, H. Dong, D. R. Baker and R. Jiang, Boosted Oxygen Evolution Reactivity by Igniting Double Exchange Interaction in Spinel Oxides, *J. Am. Chem. Soc.*, 2019, **142**, 50-54.

11 Y. Zhou, Z. Wang, Z. Pan, L. Liu, J. Xi, X. Luo and Y. Shen, Exceptional Performance of Hierarchical Ni-Fe (hydr)oxide@NiCu Electrocatalysts for Water Splitting, *Adv. Mater.*, 2019, **31**, e1806769.

12 J. Guan, C. Li, J. Zhao, Y. Yang, W. Zhou, Y. Wang and G.-R. Li, FeOOH-enhanced bifunctionality in Ni_3N nanotube arrays for water splitting, *Appl. Catal. B-*

Environ., 2020, **269**, 118600.

13 P. Ji, H. Jin, H. Xia, X. Luo, J. Zhu, Z. Pu and S. Mu, Double Metal Diphosphide Pair Nanocages Coupled with P-Doped Carbon for Accelerated Oxygen and Hydrogen Evolution Kinetics, *ACS Appl. Mater. Interfaces*, 2020, **12**, 727-733.

14 C. Huang, Y. Zou, Y. Q. Ye, T. Ouyang, K. Xiao and Z. Q. Liu, Unveiling the active sites of Ni-Fe phosphide/metaphosphate for efficient oxygen evolution under alkaline conditions, *Chem. Commun. (Camb.)*, 2019, **55**, 7687-7690.

15 Y. Liu, S. Jiang, S. Li, L. Zhou, Z. Li, J. Li and M. Shao, Interface engineering of (Ni, Fe)S_2@MoS_2 heterostructures for synergetic electrochemical water splitting, *Appl. Catal. B-Environ.*, 2019, **247**, 107-114.

16 X. Wei, Y. Zhang, H. He, D. Gao, J. Hu, H. Peng, L. Peng, S. Xiao and P. Xiao, Carbon-incorporated NiO/Co_3O_4 concave surface microcubes derived from a MOF precursor for overall water splitting, *Chem. Commun. (Camb.)*, 2019, **55**, 6515-6518.

17 H. Yan, Y. Xie, A. Wu, Z. Cai, L. Wang, C. Tian, X. Zhang and H. Fu, Anion-Modulated HER and OER Activities of 3D Ni-V-Based Interstitial Compound Heterojunctions for High-Efficiency and Stable Overall Water Splitting, *Adv. Mater.*, 2019, **31**, e1901174.

18 K. Wan, J. Luo, C. Zhou, T. Zhang, J. Arbiol, X. Lu, B. W. Mao, X. Zhang and J. Fransaer, Hierarchical Porous Ni_3S_4 with Enriched High‐Valence Ni Sites as a Robust Electrocatalyst for Efficient Oxygen Evolution Reaction, *Adv. Funct. Mater.*, 2019, **29**, 1900315.

19 T. Kou, S. Wang, J. L. Hauser, M. Chen, S. R. J. Oliver, Y. Ye, J. Guo and Y. Li, Ni Foam-Supported Fe-Doped β-Ni$(OH)_2$ Nanosheets Show Ultralow Overpotential for Oxygen Evolution Reaction, *ACS Energy Lett.*, 2019, **4**, 622-628.

20 Z. Kang, H. Guo, J. Wu, X. Sun, Z. Zhang, Q. Liao, S. Zhang, H. Si, P. Wu, L. Wang and Y. Zhang, Engineering an Earth-Abundant Element-Based Bifunctional Electrocatalyst for Highly Efficient and Durable Overall Water Splitting, *Adv. Funct. Mater.*, 2019, **29**, 1807031.

21 L. Ji, J. Wang, X. Teng, T. J. Meyer and Z. Chen, CoP Nanoframes as Bifunctional Electrocatalysts for Efficient Overall Water Splitting, *ACS Catal.*, 2019, **10**, 412-419.

22 R. Yang, Y. Zhou, Y. Xing, D. Li, D. Jiang, M. Chen, W. Shi and S. Yuan, Synergistic coupling of CoFe-LDH arrays with NiFe-LDH nanosheet for highly efficient overall water splitting in alkaline media, *Appl. Catal. B-Environ.*, 2019, **253**, 131-139.

23 X. Li, L. Xiao, L. Zhou, Q. Xu, J. Weng, J. Xu and B. Liu, Adaptive Bifunctional Electrocatalyst of Amorphous CoFe Oxide @ 2D Black Phosphorus for Overall Water Splitting, *Angew. Chem. Int. Ed. Engl.*, 2020, **59**, 21106-21113.

24 Z. Wu, D. Nie, M. Song, T. Jiao, G. Fu and X. Liu, Facile synthesis of Co-Fe-B-P nanochains as an efficient bifunctional electrocatalyst for overall water-splitting, *Nanoscale*, 2019, **11**, 7506-7512.

25 X. Zheng, X. Han, Y. Zhang, J. Wang, C. Zhong, Y. Deng and W. Hu, Controllable synthesis of nickel sulfide nanocatalysts and their phase-dependent performance

for overall water splitting, *Nanoscale*, 2019, **11**, 5646-5654.

26 J. T. Ren, G. G. Yuan, C. C. Weng, L. Chen and Z. Y. Yuan, Uniquely integrated Fe-doped $Ni(OH)_2$ nanosheets for highly efficient oxygen and hydrogen evolution reactions, *Nanoscale*, 2018, **10**, 10620-10628.

27 J. Hou, B. Zhang, Z. Li, S. Cao, Y. Sun, Y. Wu, Z. Gao and L. Sun, Vertically Aligned Oxygenated-CoS_2 - MoS_2 Heteronanosheet Architecture from Polyoxometalate for Efficient and Stable Overall Water Splitting, *ACS Catal.*, 2018, **8**, 4612-4621.

28 Y. Guo, J. Tang, Z. Wang, Y.-M. Kang, Y. Bando and Y. Yamauchi, Elaborately assembled core-shell structured metal sulfides as a bifunctional catalyst for highly efficient electrochemical overall water splitting, *Nano Energy*, 2018, **47**, 494-502.

29 Z. Wang, H. Liu, R. Ge, X. Ren, J. Ren, D. Yang, L. Zhang and X. Sun, Phosphorus-Doped Co_3O_4 Nanowire Array: A Highly Efficient Bifunctional Electrocatalyst for Overall Water Splitting, *ACS Catal.*, 2018, **8**, 2236-2241.

30 Y. Zhang, Q. Shao, S. Long and X. Huang, Cobalt-molybdenum nanosheet arrays as highly efficient and stable earth-abundant electrocatalysts for overall water splitting, *Nano Energy*, 2018, **45**, 448-455.

31 K. N. Dinh, P. Zheng, Z. Dai, Y. Zhang, R. Dangol, Y. Zheng, B. Li, Y. Zong and Q. Yan, Ultrathin Porous NiFeV Ternary Layer Hydroxide Nanosheets as a Highly Efficient Bifunctional Electrocatalyst for Overall Water Splitting, *Small*, 2018, **14**, 1703257.

32 X. Xiao, D. Huang, Y. Fu, M. Wen, X. Jiang, X. Lv, M. Li, L. Gao, S. Liu, M. Wang, C. Zhao and Y. Shen, Engineering NiS/Ni_2P Heterostructures for Efficient Electrocatalytic Water Splitting, *ACS Appl. Mater. Interfaces*, 2018, **10**, 4689-4696.

33 Z. Wu, Z. Zou, J. Huang and F. Gao, Fe-doped NiO mesoporous nanosheets array for highly efficient overall water splitting, *J. Catal.*, 2018, **358**, 243-252.

34 J. Liu, D. Zhu, T. Ling, A. Vasileff and S.-Z. Qiao, S-$NiFe_2O_4$ ultra-small nanoparticle built nanosheets for efficient water splitting in alkaline and neutral pH, *Nano Energy*, 2017, **40**, 264-273.

35 J. Liu, J. Wang, B. Zhang, Y. Ruan, L. Lv, X. Ji, K. Xu, L. Miao and J. Jiang, Hierarchical $NiCo_2S_4$@NiFe LDH Heterostructures Supported on Nickel Foam for Enhanced Overall-Water-Splitting Activity, *ACS Appl. Mater. Interfaces*, 2017, **9**, 15364-15372.